Hydrodynamic Effects of Particle Chaining in Liquid-Solid Magnetofluidized Beds

Carlos F. Cruz-Fierro*
Brian P. Reed†
Joaquin Pinto-Espinoza‡
Goran N. Jovanovic**

*Instituto Tecnologico de Durango, cfcruz@orst.edu
†Oregon State University
‡Instituto Tecnologico de Durango
**Oregon State University

HYDRODYNAMIC EFFECTS OF PARTICLE CHAINING IN LIQUID-SOLID MAGNETOFLUIDIZED BEDS

Carlos Francisco Cruz-Fierro,
Instituto Tecnologico de Durango Blvd. Felipe Pescador 1830 Ote, Durango, Durango, 34080, Mexico, T: +52 (618) 829-0918, F: +52 (618) 818-4813, cfcruz@orst.edu

Brian P. Reed, Oregon State University
Joaquin Pinto-Espinoza, Instituto Tecnologico de Durango
Goran N. Jovanovic, Oregon State University

ABSTRACT

In a fluidized bed of magnetically susceptible particles, the presence of a magnetic field induces particle chaining due to interparticle magnetic forces. The particle chains offer less resistance to flow, resulting in a decrease of the drag coefficient. The change in drag coefficient as a function of hydrodynamic and magnetic operating conditions of a liquid-solid magnetofluidized bed is studied.

INTRODUCTION

When the particles in a fluidized bed are magnetically susceptible, the hydrodynamic behavior of the bed can be altered by means of an externally applied magnetic field. Some of the first studies of magnetically susceptible fluidized systems were related to the prevention of bubbles (stabilization) in gas-solid systems (1,2). Two forces of magnetic origin can be present in a magnetofluidized bed: a force attracting the particles towards the regions of stronger magnetic field (external magnetic force), and a dipole-dipole interaction (interparticle magnetic force) which can be attractive or repulsive, depending upon the relative orientation of the particles with respect to the magnetic field.

The most important effect of interparticle magnetic forces is the formation of chains and clusters of particles. The particles, magnetized in the direction of the field, attract each other along that direction, while repelling in a direction perpendicular to the field. There is a dynamic equilibrium between the chain-forming effect of interparticle magnetic forces, and the chain-breaking effect of collisions and fluid drag. The resulting solid phase usually consists of an ensemble of individual particles, chains, and even clusters of particles, depending on the local conditions of flow and magnetic field strength. These structures have a tendency to remain aligned with the applied field. Hence, the particles in the chain or cluster will experience significantly different flow fields than the free, randomly distributed, particles in the absence of the field (Figure 1).

It has been observed that, under constant fluid flow, the bed height decreases with increasing magnetic field (3,4,5). Within a given chain, the upstream particles "protect" the downstream particles from the influence of the incoming fluid, effectively reducing the viscous drag on these particles. Additionally, the space in-between chains provides a path with less resistance for the fluid. The combined effect causes the bed to begin collapsing. This, in turn, decreases the overall void fraction, thus increasing the fluid interstitial velocity until a new dynamic equilibrium is reached.

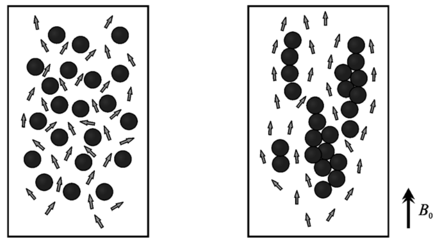

Figure 1. Difference in flow pattern through random (left) and structured (right) fluidized bed.

Current models for discrete particle simulations of fluidized beds do not take into account this change in bed structure when calculating the drag coefficient in a fluidized bed subject to a magnetic field. Rather, the drag coefficient is estimated by correlations based on the average voidage and fluid velocity in the computational cell, which typically contains at least ten particles to avoid numerical instability. The information on spatial arrangement of the particles does not affect the calculation of the drag force. In these simulations, the observed decrease in bed height and change in voidage are not predicted, affecting all calculations that depend on the hydrodynamic behavior of the bed (including any heat or mass transfer). The drag reduction factor presented in this paper is an attempt to account for the effects of interparticle magnetic force in the estimation of the drag coefficient in a fluidized bed.

THEORETICAL BACKGROUND

Governing Equations for the Continuous Phase

The dynamics of the liquid phase is governed by the mass conservation equation (1) and the momentum conservation equation (2)

$$\frac{\partial \varepsilon}{\partial t} + \nabla \cdot (\varepsilon \mathbf{u}) = 0 \tag{1}$$

$$\rho_f \frac{\partial}{\partial t}(\varepsilon \mathbf{u}) + \rho_f \nabla \cdot (\varepsilon \mathbf{u}\mathbf{u}) + \varepsilon \nabla P + \nabla \cdot (\varepsilon \tau) - \varepsilon \rho_f \mathbf{g} - \mathbf{f} = 0 \tag{2}$$

where, for a Newtonian fluid, the viscous stress tensor is given by

$$\tau = -\mu_f \left[(\nabla \mathbf{u}) + (\nabla \mathbf{u})^T \right] \tag{3}$$

Governing Equations for the Discrete Phase

Newtonian physics governs the translational and rotational motion of each individual particle, through conservation of linear momentum (4) and angular momentum (5)

$$m_P \frac{d\mathbf{v}}{dt} = \sum \mathbf{F}_i \quad (4)$$

$$I_P \frac{d\vec{\omega}_i}{dt} = \sum \mathbf{T}_i \quad (5)$$

The forces acting on the particle include gravity, buoyancy, fluid-particle interaction, particle-wall and particle-particle collisions, and magnetic forces. Fluid drag and magnetic forces are discussed further because of their relevance to this study, whereas the other forces are described elsewhere (6).

Magnetic Forces

Interparticle magnetic forces play a key role in the behavior of magnetofluidized beds. An externally applied magnetic field induces dipole magnetization on the particles. The interaction between these dipoles results in a force exerted between the particles, which can be attractive or repulsive depending on their alignment relative to the magnetic field. Because of the axial symmetry with respect to the direction of the magnetic field, the interparticle magnetic force can be expressed in a spherical coordinate system centered in one particle, split into radial and tangential components, as shown in Figure 2.

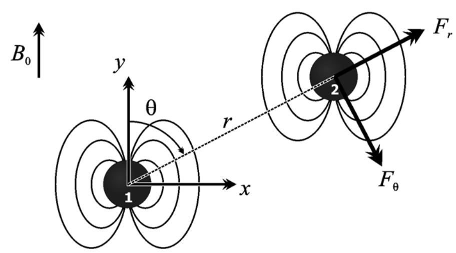

Figure 2. Spherical components of the interparticle magnetic force.

Assuming the particles as ideal dipoles whose magnetic moment depends exclusively on the externally applied magnetic field, the components of the interparticle magnetic force are given (7) as

$$F_{IM,r} = \frac{3\mu_0 |\mathbf{m}|^2}{4\pi r^4}\left(1 - 3\cos^2\theta\right) \quad \text{and} \quad F_{IM,\theta} = \frac{3\mu_0 |\mathbf{m}|^2}{2\pi r^4}\sin\theta\cos\theta \quad (6)$$

The maximum attractive force between a pair of particles occurs when the particles are in contact, aligned with the field. By setting $\theta = 0$ and $r = 2r_P = d_P$ in (7), this maximum interparticle force is

$$\left|F_{IM,\max}\right| = \frac{3\mu_0 |\mathbf{m}|^2}{2\pi d_P{}^4} \quad (7)$$

This interparticle magnetic force is present whenever a pair of magnetically susceptible particles are placed in a magnetic field. Additionally, if the magnetic field is not uniform, each dipole is attracted towards the region of strongest field. This external magnetic force is not present in the bed studied because the field is uniform.

Drag Force

The most important force between fluid and particles in a fluidized bed is the drag force. It is usually expressed in terms of a dimensionless drag coefficient, defined as

The 12th International Conference on Fluidization - New Horizons in Fluidization Engineering, Art. 46 [2007]

$$C_D \equiv \frac{\left|\mathbf{F}_D\right|}{\frac{1}{2}\rho_f \left|\mathbf{u}-\mathbf{v}\right|^2 A} \tag{8}$$

where the characteristic area is usually the particle cross sectional area, normal to the flow (8). The drag coefficient is a function of Reynolds number and geometry of the particle. The drag on a single sphere in a uniform flow field, here denoted by C_{D0}, has been subject of extensive research; for $\mathrm{Re}_P < 2' \; 10^5$ it is approximated well by the equation presented by Dallavalle (9).

$$C_{D0} = \left(0.632 + 4.8\,\mathrm{Re}_P^{-0.5}\right)^2 \quad \text{where} \quad \mathrm{Re}_P \equiv \frac{\rho_f d_P \left|\mathbf{u}-\mathbf{v}\right|}{\mu_f} \tag{9}$$

However, the drag coefficient for a spherical particle in a fluidized bed is different than that of an isolated particle, due to the effect of neighboring particles on the flow patterns around any given particle. Di Felice (10) proposed an equation for the drag coefficient applicable to fluidized and packed beds over the full practical range of Reynolds number. The drag coefficient is expressed as the product of the drag over a single particle subject to the same fluid interstitial velocity, and a voidage function

$$C_D = C_{D0}\varepsilon^{-\beta} \quad \text{where} \quad \beta = 3.7 - 0.65\exp\left[-\frac{\left(1.5-\log_{10}\mathrm{Re}_P\right)^2}{2}\right] \tag{10}$$

Correction to the Drag Force in a Magnetofluidized Bed

The magnetic drag reduction factor κ is here defined as the ratio of the drag coefficient of the particle when the magnetic field is applied relative to the drag coefficient when the field is absent

$$\kappa = \frac{C_D\big|_B}{C_D\big|_{B=0}} \tag{11}$$

and it is assumed to depend on the particle Reynolds number and on a dimensionless number, the chain strength parameter ψ, which is defined as the ratio of the maximum interparticle attractive force (7) to the particle buoyant weight

$$\psi = \frac{\left|F_{IM,\max}\right|}{\left(\rho_P - \rho_f\right) g V_P} \tag{12}$$

EXPERIMENTAL METHOD

Experimental data on bed expansion under uniform magnetic field was obtained from pressure drop measurements in a rectangular fluidized bed, constructed entirely of non-magnetizable materials. Pressure is measured with a pressure transducer (± 1.0 psi) attached to a probe that can be moved vertically to any desired location within the bed. The zone available for fluidization is 0.10 m wide, 0.05 m thick, and approximately 0.40 m high. The uniform magnetic field (up to 15.3 mT) is generated by a single coil made of 6 gauge copper wire. Particles are calcium-alginate composite beads with ferrite powder (d_P = 2.63 mm, ρ_P = 1181 kg/m³, χ_P = 0.261), fluidized with water at room temperature. Care was taken to ensure uniformity of field and flow condicions throughout the bed.

Eight different superficial velocities (between 0.0134 and 0.0482 m/s) and seven different magnetic field strengths (from zero to 0.0153 T) were tested for a total of 56 experimental runs. Under these experimental conditions, the particle Reynolds number is in the range of 75 to 190, and the chain strength parameter is in the range of 0 to 0.58.

Measurement of Drag Coefficient

In a stably fluidized bed, the pressure drop (after subtracting hydrostatic contribution) is related to the buoyant weight of the particles according to

$$\frac{dP}{dy} - \rho_f g = -(1-\varepsilon)\left(\rho_P - \rho_f\right) g \tag{13}$$

From this equation, pressure drop measurements can be used to estimate the voidage in the bed. The bed height was determined as the location above which $\varepsilon \approx 0$. A macroscopic momentum balance over the whole bed reduces to the total upward drag force balancing the total particle buoyant weight

$$\tfrac{1}{2} C_D \rho_f u^2 A N_P = \left(\rho_P - \rho_f\right) V_P g N_P \tag{14}$$

Since the fluid velocity is related to the superficial velocity and voidage as $u = u_0 / \varepsilon$, Equation 14 can be used to calculate C_D from voidage data

$$C_D = \frac{\left(\rho_P - \rho_f\right) V_P g}{\tfrac{1}{2} \rho_f \left(u_0 / \varepsilon\right)^2 A} \tag{15}$$

and then compared with the drag coefficient observed in the absence of magnetic field to obtain the (observed) drag reduction factor κ.

DISCRETE PARTICLE SIMULATIONS

The experimental conditions were replicated using Particle-X, a proprietary code for 3D CFD-DPM (Computational Fluid Dynamics-Discrete Particle Method) developed at the Chemical Engineering Department of Oregon State University. The simulation domain is discretized in rectangular fluid cells. Fluid velocity and pressure are solved using Semi-Implicit Method for Pressure-Linked Equations (SIMPLE), with first-order up-wind differencing scheme, whereas particle equations of motion are integrated using second-order Adams-Bashforth method (explicit multi-step), with time step required for collisions in the order of 10^{-4} s. The simulation includes the calculation of Interparticle magnetic forces as described in the theoretical background above.

RESULTS AND ANALYSIS

Figure 3 presents the reduction in bed height at different flow and field conditions. Figure 4 shows the relation between drag reduction factor and bed expansion. It can be noted that the effect is less pronounced at lower superficial velocities. The closer particles are, the less room they have for rearranging, so channeling and shielding effects are less pronounced. Likewise, when bed is highly expanded, the formation of chains alters much more the behavior of the dispersed phase.

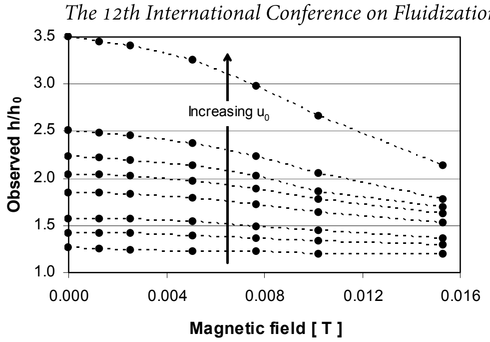

Figure 3. Change in experimental bed height with increasing magnetic field (at constant u_0).

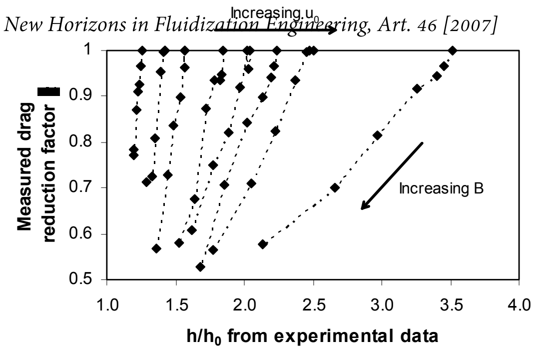

Figure 4. Change in drag reduction factor with increasing superficial velocity (u_0) and magnetic field (B). Lines connect experiments at the same u_0.

This reduction factor is correlated with particle Reynolds number and chain strength parameter using the non-linear regression model

$$\kappa = 1 - a\psi^b \, \mathrm{Re}_P{}^c \tag{16}$$

obtaining a value of R^2 of 0.94. The non-linear least-squares estimates of the three adjustable parameters and their 95% confidence interval are as follows

Parameter	Value	95% CI
a	0.06606	$\pm 9.64 \times 10^{-7}$
b	0.61160	$\pm 1.21 \times 10^{-5}$
c	0.44027	$\pm 2.99 \times 10^{-6}$

Figure 3 shows the comparison between the observed drag reduction from experimental data, and the drag reduction predicted with (16). The model provides a very good agreement with the measured values.

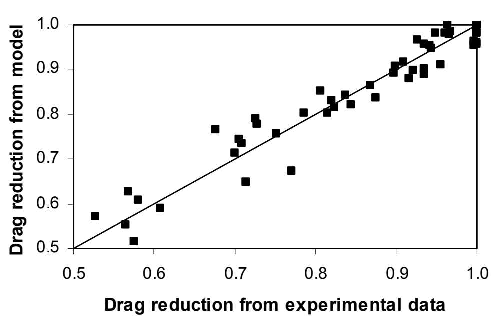

Figure 5. Agreement between experimental and predicted values of the drag correction factor.

The improvement in simulation predictions is illustrated in Figure 6. Notice the trend of overestimating the bed height when no correction is used; the worst case predicting a bed 65% more expanded than the experiment. On the other hand, using of the drag reduction factor, the worst simulation case shows an error of 8% in predicting of bed expansion.

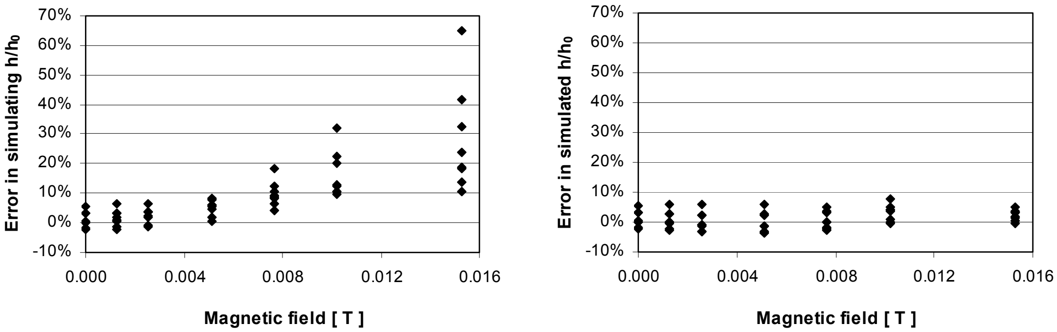

Figure 6. Comparison in error in bed expansion (relative to experimental height) when no drag correction is used (left) and when Equation 16 is used to correct the drag coefficient (right).

CONCLUSIONS AND RECOMMENDATIONS

The hydrodynamic behavior of a liquid-solid magnetofluidized bed has been studied by measuring the reduction of drag coefficient due to particle chaining. The experimental data has been reduced to the three-parameter equation

$$\kappa = \frac{C_D\big|_B}{C_D\big|_{B=0}} = 1 - 0.0661\psi^{0.612}\,\mathrm{Re}_P^{\;0.440} \tag{17}$$

which successfully describes the reduction in drag coefficient within the range of operating conditions studied, 75 < Re_P < 190 and 0 < ψ < 0.58. Additionally, incorporation of this correction into the drag coefficient in a proprietary CFD-DPM simulation code has reduced the error in bed expansion from an overestimate of up to 65% to 8% or less.

Until future research uncovers the exact nature of the drag reduction and its relation to particle chaining, this study has shown an improvement in the accuracy of simulations. The applicability of the drag reduction factor with fluidized media of different characteristics, as well as the range of applicability with respect to both parameters (Re_P and ψ) will be examined in future research. Also, the possibility of extending this concept to mixtures of particles of different properties should be examined.

ACKNOWLEDGEMENT

Financial support for this project was provided by Consejo Nacional de Ciencia y Tecnología (CONACYT, Mexico) and by the National Aeronautics and Space Administration (NASA Grant NAG9-1472).

NOTATION

A – area, [m²]
a, b, c – model parameters, [-]
$\mathbf{B}$ – magnetic field, [T]
C_D – drag coefficient, [-]
d_P – particle diameter, [m]
$\mathbf{F}$ – force, [N]
$\mathbf{f}$ – force exerted over the fluid, [N/m³]
h – bed height, [m]

h_0 – packed bed height, [m]
$\mathbf{m}$ – magnetic dipole moment, [A·m²]
m_P – particle mass, [kg]
P – fluid pressure, [Pa]
Re_P – particle Reynolds number, [-]
$\mathbf{T}$ – torque over particle, [N·m]
$\mathbf{u}$ – fluid velocity, [m/s]
V_P – particle volume, [m³]
$\mathbf{v}$ – particle velocity, [m/s]
β – voidage exponent, [-]

χ_P – particle susceptibility, [-]
ε – bed voidage, [-]
κ – drag reduction factor, [-]
μ_0 – vacuum permeability, [N/A²]
μ_f – fluid viscosity, [Pa·s]
ρ_f – fluid density, [kg/m³]
ρ_P – particle density, [kg/m³]
τ – viscous shear stress, [Pa]
ψ – chain strength parameter, [-]

REFERENCES

1. Rosensweig, R.E. *"Fluidization: Hydrodynamic Stabilization with a Magnetic Field."* Science **204** (4388) 1979. p 57-60.
2. Rosensweig, R.E. *"Magnetic Stabilization of the State of Uniform Fluidization."* Industrial and Engineering Chemistry Fundamentals **18** (3) 1979. p. 260-269.
3. Honorez, L. *"Fluid dynamic characteristics of a magnetically stabilized liquid-solid fluidized bed."* MS Thesis, Oregon State University, 1994. 81 p.
4. Pinto-Espinoza, J. *"Dynamic behavior of ferromagnetic particles in a liquid-solid magnetically assisted fluidized bed (MAFB): Theory, experiment, and CFD-DPM simulation."* PhD Thesis, Oregon State University, 2003. 271 p.
5. Villers, F. *"Bed porosity in a magnetically stabilized liquid-solid fluidized bed."* MS Thesis, Oregon State University, 1995, 79 p.
6. Crowe, C., M. Sommerfeld, and Y. Tsuji. *"Multiphase flow with droplets and particles."* CRC Press, 1997. 471 p.
7. Cruz-Fierro, C.F. *"Hydrodynamic Effects of Particle Chaining in Liquid-Solid Magnetofluidized Beds: Theory, Experiment, and Simulation."* PhD Thesis, Oregon State University, 2005. 196 p.
8. Darby, R. *"Chemical Engineering Fluid Mechanics".* Marcel Dekker, 1996. 488 p.
9. DallaValle, J.M. (1948). *"Micromeritics: The Technology of Fine Particles."* Pitman, New York, 1943.
10. Di Felice, R. *"The voidage function for fluid-particle interaction systems."* International Journal of Multiphase Flow **20** (1) 1994. p 153-159.